Accelerated healing of cutaneous wound using phytochemical-stabilized gold nanoparticles deposited hydrocolloid membrane

Journal:	*Biomaterials Science*
Manuscript ID:	BM-ART-11-2014-000390.R1
Article Type:	Paper
Date Submitted by the Author:	11-Dec-2014

Complete List of Authors:	Kim, Ji Eun; Pusan National University, Department of Biomaterials Science Lee, Jaewook; University of Calgary, Jang, Minji; Pusan National University, Nano Fusion Engineering and Cogno-Mechatronics Engineering Kwak, Moon Hwa; Pusan National University, Department of Biomaterials Science Jun, Go; Pusan National University, Department of Biomaterials Science Ko, Eunkung; Pusan National University, Department of Biomaterials Science Song, Sunghwa; Pusan National University, Department of Biomaterials Science Seong, Jieun; Pusan National University, Department of Biomaterials Science Lee, Jaebeom; Pusan National University, Hwang, Dae Youn; Pusan National University, Department of Biomaterials Science

Accelerated healing of cutaneous wound using phytochemical-stabilized gold nanoparticles deposited hydrocolloid membrane

Ji Eun Kim[1,§], Jaewook Lee[2,3,§], Minji Jang[2], Moon Hwa Kwak[1], Jun Go[1], Eun Kyoung Kho[1], Sung Hwa Song[1], Ji Eun Seong[1], Jaebeom Lee[2,**] and Dae Youn Hwang[1,*]

[1]Department of Biomaterials Science, College of Natural Resources & Life Science/Life and Industry Convergence Research Institute, Pusan National University, Miryang 627-706, Republic of Korea

[2]Department of Nano Fusion Engineering and Cogno-Mechatronics Engineering, Pusan National University, Busan 609-735, Republic of Korea

[3]Department of Mechanical and Manufacturing Engineering, University of Calgary, Calgary, T2N 1N4, Canada

[§]Both contributed equally.

***Correspondence to**: Dae Youn Hwang, Professor and Director
E-mail: dyhwang@pusan.ac.kr
Tel: +82-51-350-5388
Fax: +82-51-350-5389

****Co-correspondence to**: Jaebeom Lee, Professor
E-mail: jaebeom@pusan.ac.kr
Tel: +82-51-350-5298
Fax: +82-51-350-5299

Abstract

Rapid healing of dermatological wounds is of vital importance in preventing infection and reducing post-treatment side-effects. Here we report the therapeutic effects of phytochemical-stabilized gold nanoparticles (pAuNPs) coated on a hydrocolloid membrane (HCM) for curing cutaneous wounds. Furthermore, the remedial effects of pAuNPs on skin regeneration and angiogenesis were examined using Sprague Dawley® (SD) rats with skin injuries after a pAuNP-deposited hydrocolloid membrane (pAuNP-HCM) had been applied for 15 days. The rate of wound closure was 4 times faster in the pAuNP-HCM-treated group than in the gauze (GZ)- or HCM-treated groups in the first 5 days. Moreover, wound widths in the pAuNP-HCM-treated group were significantly reduced after 5-15 days of treatment following the injury compared with the other groups. In addition, a significant increase in collagen expression and a decrease in matrix metalloproteinase (MMP)-1 expression and transforming growth factor (TGF-β1) concentration were observed in the pAuNP-HCM-treated group on day 5. Wound tissue applied with the pAuNP-HCM showed enhancement of vascular endothelial growth factor (VEGF), angiopoietin 1 (Ang-1), and angiopoietin 2 (Ang-2) expression. Furthermore, the activity of superoxide dismutases (SODs) was significantly increased in the skin tissue of the pAuNP-HCM-treated group, compared with the GZ- or HCM-treated groups. It is probable that accelerated process of wound healing in the injured skin of SD rats via pAuNP-HCM results from the synergetic regulation of angiogenesis and connective tissue formation, as well as stimulation of antioxidant effects.

Keywords: gold nanoparticle, phytochemicals, rapid wound healing, angiogenesis, hydrocolloid membrane

Introduction

The primary function of the skin is to serve as a protective barrier against the environment. Loss of the integrity of large portions of the skin as a result of injury or illness may lead to major disability or even death. Every year in the United States more than 1.25 million people are burnt and 6.5 million have chronic skin ulcers caused by pressure, venous stasis, or diabetes mellitus.[1, 2] The primary goals of the treatment of wounds are rapid wound closure and a functional and aesthetically satisfactory scar. Rapid treatment of dermatological scar or burn wounds has indisputably impacted survival more than any other intervention.[3] Recent advances in cellular and molecular biology have greatly expanded our understanding of the biological processes involved in wound repair and tissue regeneration, and have led to improvements in wound care. However, wound healing is a complex process that can be divided into inflammatory reaction, proliferation, and maturation of newly formed tissue.[4] Even treatment of chronic wounds remains difficult, in spite of a better understanding of pathophysiological principles and greater adherence to recognized standards of care.[5] The inflammatory phase involves vascular and cellular events and is best characterized by edema, erythema, and a marked increase in blood supply. During the proliferative phase, there is formation of the epithelium with concomitant growth of granulation tissue and new blood vessels (angiogenesis). Angiogenesis seems to be strictly coordinated and regulated by multiple growth factors, chemokines, and cytokines released at the wound site.[6, 7]

Hydrocolloid membranes (HCMs), in which hydrophilic polymeric colloids are spread on a polyurethane membrane, have attracted attention in dermatological care, such as the treatment of scleroderma skin ulcers, cutaneous ulcers,[8] permanent tympanic membrane perforations,[9] pressure sores, and decubitus ulcers in the elderly.[10, 11] This is because they

have unusual characteristics such as biocompatibility and skin-friendly surfaces with high moisture absorbing capacity, and high flexibility and integrity. Milburn *et al.* studied the usefulness of HCM dressings in the treatment of finger and hand ulcers caused by scleroderma (progressive systemic sclerosis), and reported that the rate of healing of the hydrocolloid membrane-treated ulcers was significantly greater than that of the control ulcers. Pain was rapidly and dramatically reduced in all HCM-treated ulcers.[6] Gorse *et al.* also carried out a clinical study on pressure sore patients and discovered that the HCM dressing regimen was more efficacious than the wet-to-dry only dressings group. HCM treatment appears to be an effective method of accelerating healing and reducing pain. Furthermore, functional HCMs have been successfully developed by encapsulating liquids in the HCM, where the liquid contains at least one enzyme, cell, biological, immunological, or pharmaceutical agent to assist faster wound treatment.[12-14]

Essential research using AuNPs of various sizes and morphologies has been carried out in biomedical applications such as drug carriers,[15] pathogen- and tumor-targeting markers, photothermal agents,[16] and radiotheraphy dose enhancers[17, 18] owing to their unique biocompatible and physico-optical characteristics. Skin injury therapy using beneficial AuNPs is an important clinical field with great research potential. Leu *et al.,* prepared a nanocomposite mixture of AuNPs, epigallocatechin gallate (EGCG), and α-lipoic acid (ALA) to stimulate Hs68 and HaCaT proliferation and migration as well as to accelerate the wound healing of mouse skin through anti-inflammatory and antioxidant effects.[19] Chen *et al.,* reported topical application of the nanocomposite mixture of AuNPs, EGCG, and ALA to accelerate the wound healing of diabetic mouse skin and to reduce the expression of receptor for advanced glycation end-products (RAGE).[20] Furthermore, it was noticeable that a chitosan-Au nanocomposite promoted the rate of wound closure, the suppression of

inflammatory cell infiltration, the increase of capillary formation, and the formation of connective tissue.[21] Based on these essential studies on skin remedy using nanoparticles, more detailed research may be required for further medical use of AuNPs, e.g., investigations into epidermal/dermal toxicity, the wound repair process, reepithelization, and angiogenesis.

Meanwhile, as part of the functional studies on AuNPs, various phytochemical-treated AuNPs for medical applications were synthesized under non-toxic conditions.[22] It has been reported that extracts from the leaves of *Chromolaena odorata* are beneficial for the treatment of wounds. The crude ethanol extract of the plant is a powerful antioxidant capable of protecting fibroblasts and keratinocytes *in vitro*.[23] In particular, phytochemical-stabilized AuNPs (pAuNPs) were successfully produced using gallic acid, protocatechuic acid, and isoflavone, and exhibited strong antioxidant effects and excellent cytocompatibility. They were also effective reducing agents for nanomaterial synthesis.[24-26] Therefore, it is important to explore the potential of pAuNPs for new applications in human therapy.

In this study, pAuNPs were directly coated on the surface of HCM, so called, pAuNP-HCM. The therapeutic effects of pAuNP-HCM on the cutaneous wounds of Sprague Dawley® (SD) rats were examined for 15 days. In particular, the effects on the rate of wound closure, tissue regeneration, toxicity, reepithelization, angiogenesis, and antioxidant enzyme activity were carefully investigated in HCM- and pAuNP-HCM-treated rats *in vivo* (Scheme 1).

Materials and Methods

Preparation of the pAuNP-HCM

To prepare the HCM, a polymer precursor was prepared by mixing petroleum resin (200 g), gum (200 g) and tetrakis methane (6.00 g) in a hydrocolloid reactor (Young Chemical Co. Ltd,

Yangsan, Korea) for 90 min. After adding cellulose gum (210 g) and liquid paraffin (70 g), the mixture was fully dispersed to prepare a viscous polymer. The reactants were spread onto a release liner (to a thickness of 450 μm) using a knife-coater and covered with polyurethane film. Phytochemical-stabilized gold NPs (JL Nano Inc., Busan, Korea) were prepared according to J. Lee's green synthesis method[26] which is briefly described as follows: a reducing agent was prepared by mixing 10 mg isoflavone in 0.01 M of gallic acid solution (10 mL). Subsequently, 1 mL of the reducing agent was added to 0.25 mM of $HAuCl_4 \cdot 3H_2O$ solution and vigorously stirred for 30 min. The morphology was observed using transmission electron microscopy (TEM, CM-120, Philips, Eindhoven, Netherlands) at 80 kV. Next, 3.5 mL of pAuNP was dropped onto the HCM (4 × 4 cm) in a Petri dish, and shaken at room temperature at 100 rpm for 3 h to attach the pAuNPs to the HCM. After washing several times with distilled water, the pAuNP-coated HCM was dried under vacuum at 25°C.

Microscopic analysis of the pAuNP-HCM

Two membranes, one HCM and one pAuNP-HCM, were frozen at -70°C for 24 h and dehydrated for 3 days using a lyophilizer (FDU-540, Tokyo Rikakikai Co., Tokyo, Japan). After the preparation of the 2 × 2 cm dried samples, a scanned image was created using an atomic force microscope (AFM, XE-100, Park Systems Inc., Suwon, Korea). The surface morphology and surface profile were measured over an area of 30 × 30 μm and the root mean square of surface roughness (R_{RMS}) was estimated. In addition, the morphological change on each membrane was monitored by scanning electron microscopy (SEM, Stereo-scan-250-MK-III, London, UK) at 15 kV.

Design of animal experiment

The animal protocol used in this study was reviewed and approved based on ethical procedures and scientific care by the Pusan National University-Institutional Animal Care and Use Committee (PNU-IACUC; Approval Number PNU-2013-0349). Adult SD rats were purchased from SamTacho (Osan, Korea) and were given a standard irradiated chow diet (Purina Mills, Korea) *ad libitum*. All the animals were handled at the Pusan National University Laboratory Animal Resources Center accredited by the Korea Food and Drug Administration (Accredited Unit Number; 00231), and AAALAC International (Accredited Unit Number; 001525). All rats were maintained in a specific pathogen-free state under a strict light cycle (light on at 06:00 am and off at 18:00 pm) at a temperature of 22℃ and at 10% relative humidity.

Eight-week-old SD rats (n = 18) were assigned to one of three groups: a gauze (GZ)-treated group (n = 6); a HCM-treated group (n = 6); and a pAuNP-HCM-treated group (n = 6). First, animals were anesthetized by intraperitoneal injection with Zoletile (50 mg/kg body weight) and Rompun (5 mg/kg body weight). The backs of the SD rats were shaved with an electrical clipper after application of 70% ethanol. A round wound of 8 mm diameter and 2–4 mm depth was formed by removing the cutaneous tissue in the shoulder region using a biopsy punch (Kasco com, Sialkot, Pakistan). After incision, the wounds of the rats in the first group were covered with HCM, while those of the second group were covered with pAuNP-HCM. The third group received a sterilized GZ as a control. After sterilization with 70% ethanol, the incision wound on each rat was covered with a 5 × 5 × 0.3 mm piece of GZ, HCM, or pAuNP-HCM. The pieces of GZ, HCM, and pAuNP-HCM were replaced every 24 h with new pieces. During the replacement, the condition of the wound skin was observed and a photo was taken. After 2 weeks all rats were subjected to euthanasia using carbon dioxide,

and the samples of damaged skin were collected for further histological analysis, a western blot analysis, and superoxide dismutases (SODs) activity analysis.

Histological analysis

The wound tissues were removed from the SD rats of each group, fixed with 10% formalin, embedded in paraffin wax, routinely processed, and sectioned into 5 μm thick slices. The skin sections were then stained with hematoxylin and eosin (H&E, Sigma-Aldrich, MO, USA) and examined by optical microscopy (Leica Microsystems, Switzerland) for changes in skin structure. Furthermore, the diameter of the wound size and the thickness of the epidermis were measured using a Leica Application Suite (Leica Microsystems, Wetzlar, Germany).

Serum biochemical analysis

Fifteen days after the surgical wounds were administered, all the rats were fasted for 8 h, after which blood was collected from the abdominal veins and incubated for 30 min at room temperature. Serum was obtained by blood centrifugation. Serum biochemical components including alkaline phosphatase (ALP), alanine aminotransferase (ALT), aspartate aminotransferase (AST), lactate dehydrogenase (LDH), blood urea nitrogen (BUN), and creatinine (CR) were assayed using an automatic serum analyzer (HITACHI 747, Tokyo, Japan). All assays were measured using fresh serum and conducted in duplicate.

Western blot

Wound skins from a subset of the groups (n = 5 per group) were homogenized using a PRO-PREP^{TM} solution kit (iNtRON Biotechnology, Sungnam, Korea) supplemented with 1/2 of a protein inhibitor cocktail tablet (Roche, Penzberg, Germany), followed by centrifugation

at 13,000 rpm for 5 min. The prepared proteins were then electrophoresed through a 10% sodium dodecyl sulfate polyacrylamide gel electrophoresis (SDS-PAGE) gel. The proteins were then transferred onto a nitrocellulose membrane (Amersham Biosciences, Corston, UK) for 2 h at 40 V in a transfer buffer (25 mM Trizma-base, 192 mM glycine, and 20% methanol). The efficiency of the transfer and equal protein loading were determined by staining the gel with Coomassie Blue (Sigma-Aldrich, MO, USA). Appropriate dilutions of primary antibodies, anti-collagen antibody (Abcam Inc., Cambridge, MA, USA), anti-matrix metalloproteinase-1 (MMP-1) antibody (Santacruz Biotechnology, Santa Cruz, CA, USA), anti-vascular endothelial growth factor (VEGF) antibody (Pepro Tech., NJ, USA), anti-Ang-1 antibody (Santacruz Biotechnology, Santa Cruz, CA, USA), anti-Ang-2 antibody (Santacruz Biotechnology, Santa Cruz, CA, USA) and anti-β-actin antibody (Sigma-Aldrich, MO, USA) were added to the membranes and allowed to hybridize overnight at 4℃. After the antibodies were removed, the membranes were washed 3 times in a solution consisting of 10 mM Trizma-base (pH 7.6), 150 mM NaCl, and 0.05% Tween-20 for 10 min. This was followed by incubation with horseradish peroxidase (HRP)-conjugated anti-secondary antibody for 1 h at room temperature. The membrane was washed again as described above and developed using an enhanced chemiluminescence detection system (Amersham Bioscience). Finally, the density of each band was quantified using an image analyzer system (Eastman Kodak 2000MM, NY, USA) and expressed as a fold-increase over control value. All results were confirmed by two independent researchers who performed the experiments at least twice.

Immunohistochemical analysis

Immunohistochemical analysis was performed as previously described.[27] Briefly, the distribution of collagen and MMP-1 protein was observed by optical microscopy after fixing the tissue samples in 5% formalin for 48 h, embedding the tissues in paraffin, and acquiring 3 μm thick sections. Each section was de-paraffinized with xylene, rehydrated, and pretreated for 30 min at room temperature with a phosphate buffered saline (PBS)-based blocking buffer containing 10% goat serum. The samples were then incubated with mouse anti-collagen antibody (Abcam Inc., Cambridge, MA, USA) and anti-MMP-1 antibody (Santacruz Biotechnology, Santa Cruz, CA, USA) diluted 1:1000 in PBS-blocking buffer. Antigen-antibody complexes were visualized with goat anti-rabbit HRP-conjugated streptavidin secondary antibody (Histostain-Plus Kit, Zymed Laboratories) diluted 1:1000 in PBS-blocking buffer. Collagen and MMP-1 proteins were detected using a 3,3′-diaminodbenzidine (DAB) substrate (Invitrogen, Carlsbad, CA, USA) and a model GS-690 imaging densitometer (Bio-Rad Laboratories, Hercules, CA, USA).

Enzyme-linked immunosorbent assay (ELISA) for transforming growth factor (TGF-β1)

The concentrations of total TGF-β1 in serum were measured using the Legend Max Total TGF-β1 ELISA kit (BioLegend, San Diego, CA) according to the manufacturer's instructions. Briefly, the capture antibody-coated wells in Nunc C bottom immunoplates supplied in the kit were washed 3 times with washing solution. The serum samples and standards were added to the wells, and the plates were incubated at room temperature for 2 h. After washing 3 times, TGF-β1 detection antibody solution was added into each well and incubated at room temperature for 1 h with shaking. The wells were then washed with washing solution, after which HRP-conjugated detection antibodies were diluted 5,000 fold with conjugate diluent

(50 mM Tris, 0.14 M NaCl, 1% BSA, 0.05% Tween 20, pH 8.0) and transferred to each well. The plates were incubated at room temperature for 30 min, after which they were washed 3 times with washing solution. An enzyme reaction was initiated by adding substrate solution and incubating the plate at room temperature in the dark for 30 min. Finally, the reaction was terminated by adding a stop solution, and the absorbance at 450 nm was measured within 30 min using a microplate reader (Molecular Device, USA).

Activity analysis of superoxide dismutases (SODs)

The SODs activity in the wound skin was detected using the calorimetric assay procedure and the reagents in a SOD assay kit (Dojindo Molecular Technologies, Inc., Japan). The skin tissue (100 mg) was homogenized in 600 μL of sucrose buffer (0.25 mol/L sucrose, 10 mmol/L 4-(2-hydroxyethyl)-1-piperazineethanesulfonic acid (HEPES), 1 mmol/L ethylenediaminetetraacetic acid (EDTA), pH 7.4) using a glass homogenizer. The lysate was harvested from the mixture by centrifugation at 10,000 × *g* for 60 min and stored at -70°C until required for the enzyme activity assay. To measure the SODs activity, the sample lysate was serially diluted with dilution buffer or saline as follows; 1, 1/5, $1/5^2$, $1/5^3$, $1/5^4$, $1/5^5$ and $1/5^6$ ratio. A 25 μL aliquot of the sample solution was added to each well of a 96-well plate for blank or sample. To this was added 200 μL of a water-soluble tetrazolium (WST) working solution that comprised WST-1 [2-(4-iodophenyl)-3-(4-nitrophenyl)-5-(2,4-disulfophenyl)-2H-tetrazolium, monosodium salt] and produced a water-soluble formazan dye upon reduction with a superoxide anion. In addition, 20 μL of enzyme working solution was added to each sample and mixed thoroughly. The enzyme reaction was induced by incubation of the mixture plate at 37°C for 20 min and the absorbance was measured by a UV-Vis spectrophotometer at 450 nm. The SODs activity was calculated directly using the following

equation: SODs activity (Inhibition rate %) = [(S1-S2) - (SS-S2)] / (S1-S2) × 100 (S1: slope of blank 1, S2: slope of blank 2, S3 : slope of blank 3, SS : slope of sample).

Statistical analysis

One-way analysis of variance (ANOVA) tests (SPSS for Windows, Release 10.10, Standard Version, Chicago, IL) were performed to determine the variance and significance between the GZ group and the other treated groups. In addition, the tests for significance between the HCM- and pAuNP-HCM-treated groups were performed using a post-hoc test of the variance (SPSS for Windows, Release 10.10, Standard Version, Chicago, IL), and the significance levels are given in the text. All values were reported as the mean ± standard deviation (SD). A p-value of < 0.05 was considered significant.

Results and Discussion

Surface morphology of HCM and pAuNP-HCM

The average length of the pAuNPs with hexagonal morphology of 1:1~1:1.5 aspect ratio was -30 nm and they were well dispersed in aqueous solution (Figure 1Aa). It has been reported that these NPs have excellent biocompatibility and low cytotoxicity in dense concentration (up to 50 μg/mL) and are probably suitable for further biological applications.[8] The surface morphology of each condition of the HCMs, i.e., before/after coating with pAuNPs, was observed using AFM and SEM. In the AFM images of Figure 1Ac-d, each surface of the different HCM samples shows unique morphologies depending on pAuNP coating. The non-coated HCM sample shows higher roughness than the pAuNP-coated HCM sample, resulting in higher R_{RMS}: 382 nm and 76 nm, respectively (Figure 1Ab). The SEM images in Figure 1B reveal that the copious quantities of pAuNPs deposited on the surface of

the HCM produced a different surface morphology, which probably affected cell growth and therapeutic effect.

Effect of pAuNP-HCM treatment on wound healing rate

To determine how stimulation with pAuNP-HCM affected the closing process of the wound skin, the closing rate of the wound area was measured for the skin that was covered with the pAuNP-HCM. A round area of 8 mm diameter and 2–4 mm depth was covered by each of GZ, HCM, and pAuNP-HCM and monitored for 15 days. We noticed that the most significant changes in the wound area occurred within the first 5 days. The wound closing area was carefully measured. In the pAuNP-HCM sample, the diameter of the wound area decreased to 1.6 cm from 2.0 cm, while that of the HCM sample showed only a 0.1 cm change in the same period. In other words, the wound closing rate was 4 times faster in the pAuNP-HCM sample than in the non-coated HCM sample during the first 5 days. The closing rate of the pAuNP-HCM sample remained the fastest of the samples until the final observation after 15 days, at which point the wound skin was completely repaired in all treated groups (Figure 2). Therefore, these results suggest that the skin's enhanced ability to heal the wound and regenerate tissue could be reasonably attributed to pAuNP-HCM.

Effect of pAuNP-HCM treatment on the tissue regeneration of wound skin

The closing rate of the wound area was determined based on the recovery of the epidermis, dermis, and hyperdermis of the skin tissue of the rats over the designated duration (i.e., 5, 10, and 15 days). To examine the therapeutic effects of the pAuNP-HCM on the histological structure of burns on the skin, the wound length and the thickness of the epidermis and dermis were monitored in the GZ-, HCM-, and pAuNP-HCM-treated rats. After the first 5

post-surgery days, the wound length was significantly reduced by about 35.7% in the pAuNP-HCM-treated group compared with the GZ-treated group, while it was maintained at a constant level in the HCM-treated group. After 10 days post-surgery, both the HCM- and pAuNP-HCM-treated groups had shorter wound lengths than the GZ-treated group, although a larger decrease was detected in the pAuNP-HCM-treated group. This pattern was also detected at 15 days post-surgery; nevertheless, the rate of change was distinguishable between the two time points (Figure 3A and B). In addition, the recovery of the epidermis was first detected at 5 days post-surgery in the HCM- and pAuNP-HCM-treated groups, but did not appear until 15 days post-surgery in the GZ-treated group. Furthermore, the number of blood vessels in the dermis was gradually increased from the 5^{th} day to the 15^{th} in the pAuNP-HCM-treated group (Figure 3A). Therefore, these results suggest that pAuNP-HCM treatment could improve tissue regeneration including decreasing wound length, formation of blood vessels, and recovery of the epidermis in the skin tissue of SD rats.

Toxicity of pAuNP-HCM

To investigate pAuNP-HCM toxicity in the livers and kidneys of SD rats, the alteration of several enzymes related to liver and kidney metabolism was investigated in blood serum using serum biochemical analysis. In the liver toxicity analysis, there were no increase in the levels of four liver toxicity indicators, specifically ALP, AST, ALT, and LDH, between the pAuNP-HCM-treated group and the GZ-treated group at most time points, although slightly lower levels in the pAuNP-HCM-treated group were detected at day 10 and 15 (Table 1).

In the kidney toxicity analysis, similar results to those observed in the liver toxicity analysis applied to the BUN and Cr levels. The level of BUN and Cr in the serum did not significantly increase in the pAuNP-HCM-treated rats, regardless of the exposure time. However, the level

of BUN was slightly lower at two time points in the AuNP-HCM-treated groups (Table 1). Therefore, these results indicate that topical application of pAuNP-HCM and infusion into the subcutaneous region for 15 days does not induce any toxicity in the liver or kidney of SD rats.

Effect of pAuNP-HCM on the formation of connective tissue in the wound skin

To evaluate the effects of pAuNP-HCM treatment on the formation of connective tissue in the wound skin, we measured the expression level of collagen and MMP-1 in a subset of groups for different times. The expression level of collagen was significantly higher in the pAuNP-HCM-treated group relative to that in the GZ- or HCM-treated groups at 5 days post-surgery, although this level rapidly decreased over time. However, the HCM-treated group showed a slightly increased level at 10 days post-surgery, while the GZ-treated group maintained a constant level of collagen expression. At 15 days post-surgery no significant difference was detected between the treated groups (Figure 4A-C).

The next step was to determine whether overexpression of collagen was accompanied by a decrease in the expression of collagen-degrading enzyme, so the expression levels of MMP-1 were measured in a subset of the groups. The pattern of MMP-1 expression at 5 days post-surgery was very similar to the reverse of the results for collagen expression, while expression at 10 and 15 days post-surgery resembled the expression of collagen. The intensity of MMP-1 expression was lowest in the pAuNP-HCM-treated group compared with that in the GZ- or HCM-treated groups, while the HCM-treated group evidenced a similar level of MMP-1 expression to the GZ-treated group. However, at 10 or 15 days post-surgery MMP-1 expression in each group was very similar to that of collagen (Figure 4A-C). Furthermore, the concentration of TGF-β1, which regulates the expression of MMP-1 and MMP-13, was

significantly reduced in the pAuNP-HCM-treated group compared with the GZ- or HCM-treated groups at 10 and 15 days post-surgery (Figure 4D). Overall, these findings indicate that pAuNP-HCM treatment may induce an increase of collagen through the suppression of MMP-1 expression at the early stage of the wound skin repair process.

The relationship between pAuNP-HCM and angiogenesis in the wound skin

Generally, tissue regeneration is coupled with vascular regeneration, which includes the restoration of normal vascular function and structure, the reversal of vascular senescence, and the growth of new blood vessels.[28] To determine whether pAuNP-HCM treatment induces an alteration in the vascular regeneration of wound skin, the expression levels of angiogenesis stimulators were measured using western blot analysis in a subset of the group. The expression level of VEGF in the GZ- and HCM-treated groups gradually decreased over time, while in the pAuNP-HCM-treated group it rapidly decreased at 15 days post-surgery after a large increase at 10 days post-surgery (Figure 5). However, a significant alteration in the expression of Ang-1 was only detected after 15 days, and not at 5 or 10 days post-surgery. At 15 days, the level was higher in the pAuNP-HCM-treated group than in the GZ- or HCM-treated groups, although it was slightly higher in the HCM-treated group than in the GZ-treated group (Figure 5). Furthermore, in the case of Ang-2 expression, a similar pattern with a gradual increase was observed in the GZ- and HCM-treated groups, while a different level was detected in the pAuNP-HCM-treated group, in which, in particular, the level increased to a maximum at day 10 after skin injury. Therefore the data suggest that pAuNP-HCM treatment may significantly accelerate angiogenesis through the differential regulation of related protein expression.

Effect of pAuNP-HCM on SODs activity

Finally, to examine the possible roles of pAuNP-HCM treatment in the wound environment, SODs activity was measured in the wound skin of GZ-, HCM-, and pAuNP-HCM-treated rats. There was no difference in the level of SODs activity among the three groups at day 5 after skin injury. However, at days 10 and 15, the activity was significantly higher in the pAuNP-HCM-treated group than in the GZ- or HCM-treated groups, although it did increase in the HCM-treated group compared with the GZ-treated group (Figure 6). These results indicate that pAuNP-HCM treatment could inhibit oxidative stress after cutaneous injury of SD rats.

Discussion

Gold nanoparticles have recently received increased attention as a novel tool for many medical applications including the diagnosis for various diseases, therapy for several chronic and acute diseases, and research in immunology and biodistribution.[29] In an effort to develop and investigate a wound dressing for application to cutaneous wound skin, we investigated the therapeutic effects of pAuNP-HCM on skin injury in SD rats. The results clearly demonstrate that pAuNP-HCM has wound healing properties, including increasing wound closure rate, rapidly decreasing wound length, non-toxicity, connective tissue formation and increasing angiogenesis activity. Our data are the first to demonstrate that pAuNPs coated on the surface of HCM successfully induce the regeneration and re-epithelization of wound skin through the inhibition of oxidative stress after surgical injury.

This study found that pAuNP-HCM treatment had effects on the stimulation of wound closure in the injured skin of SD rats. Increase of wound closure rate, as well as regeneration of normal tissue including decrease of wound width, were strongly detected within 15 days of

surgical injury. This result was consistent with previous reports that topical application of AuNPs + epigallocatechin gallate + α-lipoic acid (AuEA) significantly increased the rate of wound healing over that of vehicle groups in normal or diabetic BALB/c mice. Furthermore, in the histological section of a skin sample from the AuEA-treated group, inflammation and neutrophil infiltration were limited to the site of cutaneous wound skin on day 7.[19] Also, wound widths and lengths were significantly decreased from the 5th to the 7th days after injury compared with the vehicle-treated group.[20] Chitosan nanocomposites prepared from chitosan and AuNPs promoted the rate of healing closure, the decrease of inflammatory cells, the increase of capillary formation, the disappearance of hyperemia in microvessels, and the formation of connective tissue.[23] We speculate that pAuNP-HCM successfully stimulates the regeneration of wound skin in SD rats. However, more studies are needed to investigate whether pAuNP-HCM can induce the therapeutic effects in the wound skin of diabetic rats.

Generally, adverse effects and toxicity of nanoparticles in humans are determined by individual factors such as pre-existing disease and genetics, exposure dose and time, and nanoparticle properties including chemistry, size, shape, agglomeration state, and electromagnetic properties.[27] When 10 and 50 nm AuNPs are intraperitoneally administered to rats for 3 days, the increase in AST and the decrease in ALP are induced by the smaller AuNPs, while a decrease in GGT and ALT is induced by the bigger AuNPs. The levels of urea and Cr indicate no significant changes after administration of 10 and 50 nm AuNPs over 3 days.[30] However, the repeated intraperitoneal injection of AuNPs at a dose of 10 mg/kg three times a week, up to 20 injections, did not induce any significant alteration in the level of indicator enzymes for liver (ALP, AST and ALT) or kidney (Cr and BUN) toxicity.[31] Furthermore, no significant differences were found between the control and any treated group in the level of indicator enzymes for liver and kidney toxicity when SD rats were exposed to

AuNPs with average diameter 4–5 nm for 6 h/day, 5 days/week, for 90 days in a whole-body inhalation chamber.[32] Moreover, pAuNPs used in that study produced no noticeable dose-dependent decrease in the viabilities of L-929 fibroblastic cells. In our study, the level of most indicators for liver and kidney toxicity were maintained at a constant level during all experimental periods, although LDH level was slightly reduced at day 5. These results are in complete agreement with the observation that AuNP treatment does not correlate with liver and kidney toxicity, although they only partially agree with the results reported by Abdelhalim and Abdelmottaleb Moussa.[30] We think that these differences between studies can be attributed to the chemical properties of AuNPs, and the differences in method and time of application. Our results show that the cutaneous application of pAuNPs onto the wound skin for 15 days does not induce liver or kidney toxicity.

Angiogenesis may play an important role in wound healing through producing microvessels that transport nutrients and oxygen to growing dermal cells.[33] Animal studies have shown that several different forms of AuNP stimulate angiogenesis in wound skin through the regulation of related protein expression. Immunoblotting of wound tissue from AuEA-treated mice showed a significant increase of VEGF and Ang-1 expression, but no change of Ang-2 after 7 days.[19] However, in diabetic mice the pattern of expression was different. VEGF, but not Ang-1, significantly increased in the AuEA-treated group at day 7, while Ang-2 was reduced in the same group.[20] In addition, enhancement of capillary formation was observed in the chitosan nanocomposite-treated group compared with the control group.[26] In this study, the expression of three proteins related to angiogenesis partially agreed with previous results. In particular, the data from VEGF and Ang-1 in our study are completely in accord with their expression in the skin of the non-diabetic AuEA-treated group, while Ang-2 expression had the same pattern only in diabetic subjects. Therefore,

these results suggest that angiogenesis is accelerated by several types of pAuNP, although their mechanism is controlled differently through the up- or down-regulation of related proteins.

It is well recognized that SODs play an important part in the first line of cellular defense against free radical species. Also, they specifically catalyze the superoxide radical into oxygen and hydrogen peroxide by a dismutation process. The levels of antioxidant defense enzymes, including SODs, were significantly increased in the diabetic mice treated with a dosage of 2.5 mg/kg.b.wt/day of AuNP for 45 days.[34] Also, treatment with citrate-capped AuNPs induced the enhancement of SODs and CAT levels in MCF-7 and HepG2 cell lines,[35] while AuEA treatment increased the expression of SODs in both normal and diabetic BALB/c mice. An excellent antioxidant effect of up to 40% was exhibited by pAuNPs at the affordable biocompatibility of NPs.[32] In our study, the alteration of SODs level was very similar to the results from most of the studies mentioned above, although different methods have been applied to measure SODs activity and expression. SODs activity was higher in the pAuNP-HCM-treated group than in the GZ- or HCM-treated groups at days 10 and 15 post-surgery, as shown in Figure 6. Therefore, these results provide additional evidence for the correlation between SODs activity and pAuNP-HCM in the wound healing process.

Conclusion

We have demonstrated clearly that topical application of pAuNP-HCM for 15 days induces the acceleration of wound healing including tissue regeneration, connective tissue formation, and angiogenesis. Moreover, our study provides insight into the molecular action of pAuNP-HCM in a cutaneous wound healing model of SD rats. This study also shows that pAuNP-HCM may not induce any significant toxicity in the liver or kidney of rats. Therefore, our

results provide a rationale for the future development of pAuNP-HCM with other antioxidants in topical applications for cutaneous wounds.

Acknowledgments

This study was supported by a grant of the Korean Health Technology R&D Project, Ministry of Health & Welfare, Republic of Korea (HI13C0862); and Basic Science Research Program through the National Research Foundation of Korea (NRF) funded by the Ministry of Education (2013004637).

Reference list

1. A. T. Vidimos, *Dermatologic Surgery*, Philadelphia, 2009.
2. F. H. Epstein, A. J. Singer and R. A. Clark, *New England journal of medicine*, 1999, **341**, 738-746.
3. N. S. Gibran, S. Boyce and D. G. Greenhalgh, *Journal of burn care & research*, 2007, **28**, 577-579.
4. C. Baum, and CJ. Arpey *Dermatologic surgery*, 2005, **31**, 674-686.
5. J. a. V. F. Cha, *Clinics in dermatology*, 2007, **25**, 73-78.
6. P. B. Milburn, J. Z. Singer and M. A. Milburn, *Journal of the American Academy of Dermatology*, 1989, **21**, 200-204.
7. J. Yoon, J. Giacopelli, D. Granoff and W. Kobayashi, *Journal of the American Podiatric Medical Association*, 2002, **92**, 350-354.
8. A. Chakrabarty, and T. Phillips, *The international journal of lower extremity wounds*, 2003, **2**, 207-216.
9. O. Spandow, S. Hellstrom, M. Dahistrom and L. Bohlin, *The Journal of Laryngology & Otology*, 1995, **109**, 1041-1047.
10. G. J. Gorse, and R. L. Messner, *Archives of dermatology*, 1987, **123**, 766.
11. C. Honde, C. Derks and D. Tudor, *Journal of the American Geriatrics Society*, 1994, **42**, 1180-1183.
12. *USA Pat.,* US5486158 A, 1996.
13. *USA Pat.,* US20030092969 A1, 2003.
14. *USA Pat.,* US6680184 B2, 2004.
15. J. D. Gibson, B. P. Khanal and E. R. Zubarev, *Journal of the American Chemical Society*, 2007, **129**, 11653-11661.
16. C. P. Liu, Lin F.S., C. Chien, S. Tseng, C.W. Luo, C.H. Chen, J.K. Chen, F.G. Tseng, Y. Hwu, L.W. Lo, C.S. Yang, and S.Y. Lin, *Macromolecular bioscience*, 2013, **13**, 1314-1320.
17. J. F. Hainfeld, F. A. Dilmanian, Z. Zhong, D. N. Slatkin, J. A. Kalef-Ezra and H. M. Smilowitz, *Physics in medicine and biology*, 2010, **55**, 3045.
18. J. F. Hainfeld, D. N. Slatkin and H. M. Smilowitz, *Physics in medicine and biology*, 2004, **49**, 309.

19. J. G. Leu, S. A. Chen, H. M. Chen, W. M. Wu, C. F. Hung, Y. D. Yao, C. S. Tu and Y. J. Liang, *Nanomedicine: Nanotechnology, Biology and Medicine*, 2012, **8**, 767-775.
20. S. A. Chen, H. M. Chen, Y. D. Yao, C. F. Hung, C. S. Tu and Y. J. Liang, *European Journal of Pharmaceutical Sciences*, 2012, **47**, 875-883.
21. S. h. Hsu, Y. B. Chang, C. L. Tsai, K. Y. Fu, S. H. Wang and H. J. Tseng, *Colloids and Surfaces B: Biointerfaces*, 2011, **85**, 198-206.
22. J. Lee, E. Y. Park and J. Lee, *Bioprocess and Biosystems Engineering*, 2014, **37**, 983-989.
23. T. Phan, Wang L, See P, Grayer RJ, Chan SY, and Lee ST., *Biological & pharmaceutical bulletin*, 2001, **24**, 1373-1379.
24. J. Lee, R. A. Syed, S. J. Oh, J. H. Kim, T. Suzuki, K. Parmar, S. S. Park, J. Lee and E. Y. Park, *Biosensors and Bioelectronics*, 2015, **64**, 311-317.
25. J. Lee, J. H. Kim, S. Rahin Ahmed, H. Zhou, J. M. Kim and J. Lee *ACS Applied Materials & Interface*, 2014, **4**, 313-317.
26. J. Lee, H. Y. Kim, H. Zhou, S. Hwang, K. Koh, D. W. Han and J. Lee, *Journal of Materials Chemistry*, 2011, **21**, 13316-13326.
27. C. Buzea, I. I. Pacheco and K. Robbie, *Biointerphases*, 2007, **2**, MR17-MR71.
28. N. J. Leeper, A. L. Hunter and J. P. Cooke, *Circulation*, 2010, **122**, 517-526.
29. L. Dykman, and N. Khlebtsov, *Chemical Society Reviews*, 2012, **41**, 2256-2282.
30. M. A. Abdelhalim, and S. A. Abdelmottaleb Moussa, *Saudi journal of biological sciences*, 2013, **20**, 177-181.
31. B. A. Katsnelson, L. I. Privalova, V. B. Gurvich, O. H. Makeyev, V. Y. Shur, Y. B. Beikin, M. P. Sutunkova, E. P. Kireyeva, I. A. Minigalieva and N. V. Loginova, *International journal of molecular sciences*, 2013, **14**, 2449-2483.
32. J. H. Sung, J. H. Ji, J. D. Park, M. Y. Song, K. S. Song, H. R. Ryu, J. U. Yoon, K. S. Jeon, J. Jeong and B. S. Han, *Part Fibre Toxicol*, 2011, **8**, 16.
33. E. Andrikopoulou, X. Zhang, R. Sebastian, G. Marti, L. Liu, M. Milner and W. Harmon, *Current molecular medicine*, 2011, **11**, 218-235.
34. S. BarathManiKanth, K. Kalishwaralal, M. Sriram, S. R. K. Pandian, H. s. Youn, S. Eom and S. Gurunathan, *Journal of Nanobiotechnology*, 2010, **8**.

35. S. Ito, N. Miyoshi, W.G. Degraff, K. Nagashima, L.J. Kirschenbaum and P. Riesz, *Free radical research*, 2009, **43**, 1214-1224.

Scheme Legend

Scheme 1. Illustration of pAuNP-HCM preparation and skin damage treatment process (non-scalable)

Figure Legends

Figure 1. Morphology of pAuNP and AuNP-HCM. (Aa) The structure and shape of pAuNP was observed by transmittance electron microscopy at magnification 50,000x. In addition, the morphological image on the surface of HCM and pAuNP-HCM was collected with AFM (A-c and d) and SEM analysis (B). In AFM analysis, 3D-images of HCM and pAuNP-HCM on the form were analyzed in 25 μm^2 scan size (3 x 3 μm). (Ab) The roughness on the surface of HCM and pAuNP-HCM were calculated from the AFM data. Data represent the mean ± SD from three replicates. a, $p < 0.05$ is the significance level compared to HCM. Ultrastructure on the surface of HCM and AuNP-HCM was observed with SEM at magnification 10,000x as described in Materials and Methods. Three to five membranes per group were assayed in duplicate by SEM analysis.

Figure 2. Closing pattern of wound skin as time passes. A round wound of dermis was created with Biopsy Punch in the back skin of SD rats and covered with three different membranes. At each time point, the images of wound skin were taken from rats of each group and used for the calculation of wound area. Five or six wound were assayed in triplicate using wound area analysis. The values are the mean ± SD. ∗, $p < 0.05$ is the significance level compare to the GZ treated group.

Figure 3. Alteration on the histological analysis after pAuNP-HCM application. (A) H&E stained sections of subcutaneous tissue surrounding the pAuNP-HCM applied in SD rat for

different time points were observed using a light microscope at magnifications of 10x (a-i) and 400x (j-l). (B) Wound size and thickness of epidermis at the indicated time points in GZ, HCM, or pAuNP-HCM treated rats were measured using Leica Application Suite as described in Materials and methods. Data represent the mean ± SD from three replicates. *, $p < 0.05$ is the significance level compared to GZ treated group. **, $p < 0.05$ is the significance level compared to HCM treated group.

Figure 4. Effects of pAuNP-HCM on the formation of connective tissue. Expression of (B) collagen and (C) MMP-1. Wound samples were then collected from rats of each group and were subjected to western blot analysis. Data represent the mean ± SD from three replicates. *, $p < 0.05$ is the significance level compared to GZ treated group. **, $p < 0.05$ is the significance level compared to HCM treated group. (D) Concentration of TGF-1β in blood serum. ELISA kit used this experiment can detect from 7.8 pg/mL to 500 pg/mL of TGF-1β concentration. Data represent the mean ± SD from three replicates. *, $p < 0.05$ is the significance level compared to GZ treated group. **, $p < 0.05$ is the significance level compared to HCM treated group.

Figure 5. Expression of angiogenesis-related proteins in wound skin. The expression level of VEGF, Ang-1 and Ang-2 were measured using specific antibody in the cutaneous wound skin collected from rats of each group at different time point after pAuNP-HCM application. Data represent the mean ± SD from three replicates. *, $p < 0.05$ is the significance level compared to GZ treated group. **, $p < 0.05$ is the significance level compared to HCM treated group.

Figure 6. Analysis for SOD activity. After final application, wound skins were collected from rats of each group, and then SOD activity was measured using SOD Assay Kit as described in Materials and methods. Data represent the mean ± SD from three replicates. *, $p < 0.05$ is the significance level compared to GZ treated group. **, $p < 0.05$ is the significance level compared to HCM treated group.

Table Legend

Table 1. Toxicity of pAuNP-HCM in the serum of SD rats

Scheme 1.

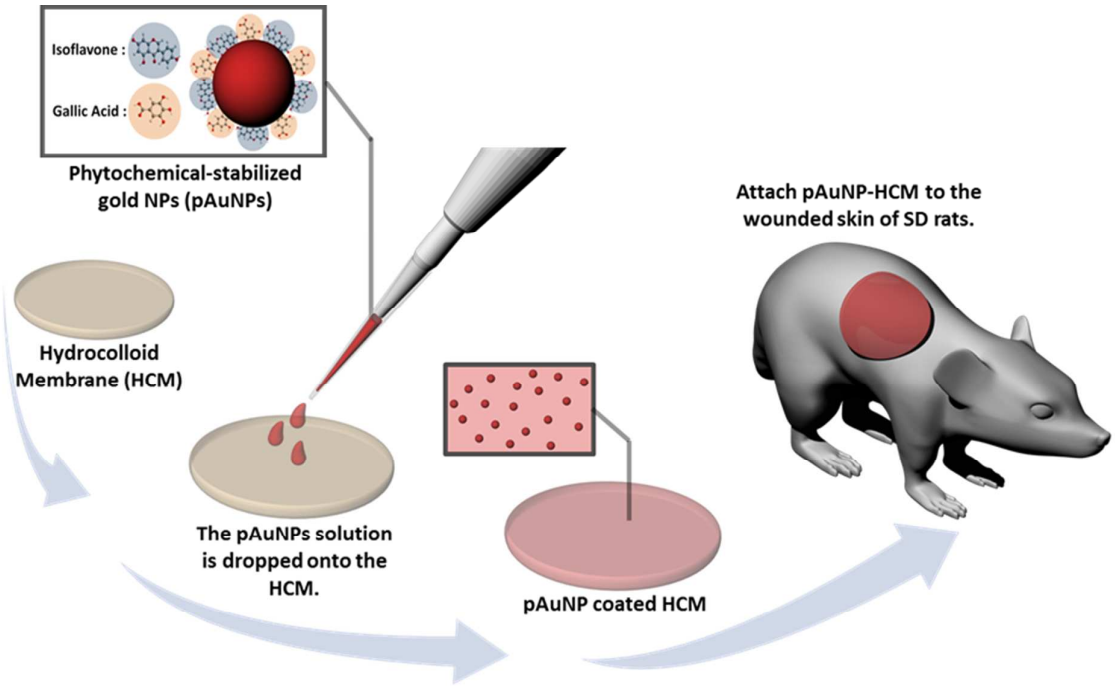
Isoflavone :
Gallic Acid :
Phytochemical-stabilized gold NPs (pAuNPs)
Hydrocolloid Membrane (HCM)
The pAuNPs solution is dropped onto the HCM.
pAuNP coated HCM
Attach pAuNP-HCM to the wounded skin of SD rats.

Figure 1

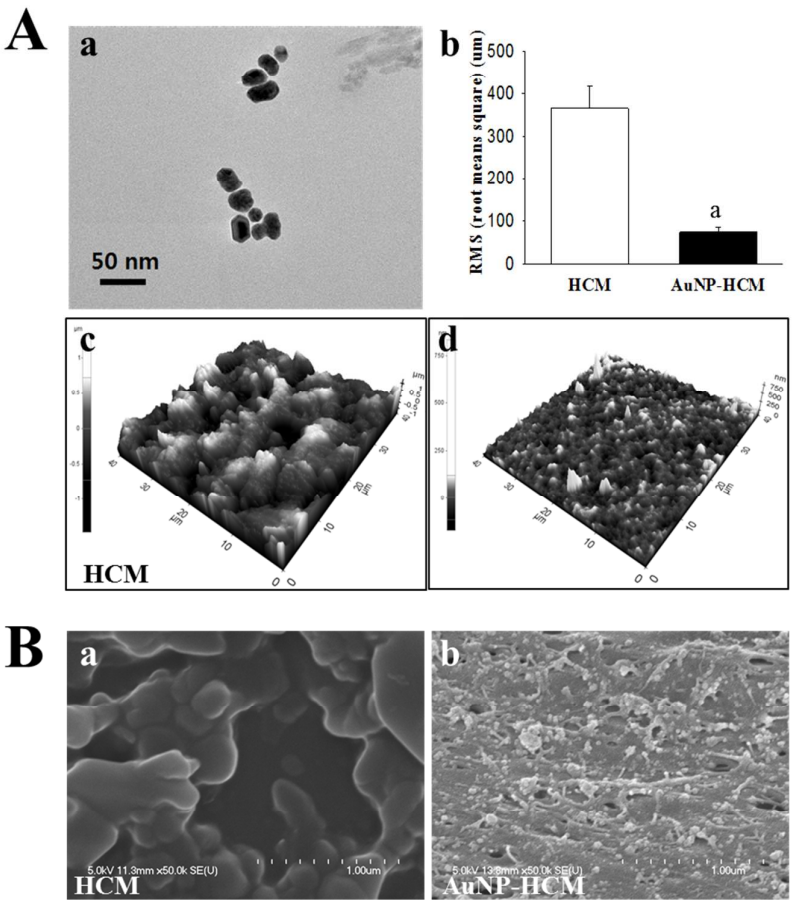
A
a
50 nm
b
RMS (root means square) (nm)
500
400
300
200
100
0
a
HCM
AuNP-HCM
c
HCM
d
B
a
HCM
b
AuNP-HCM

Figure 2

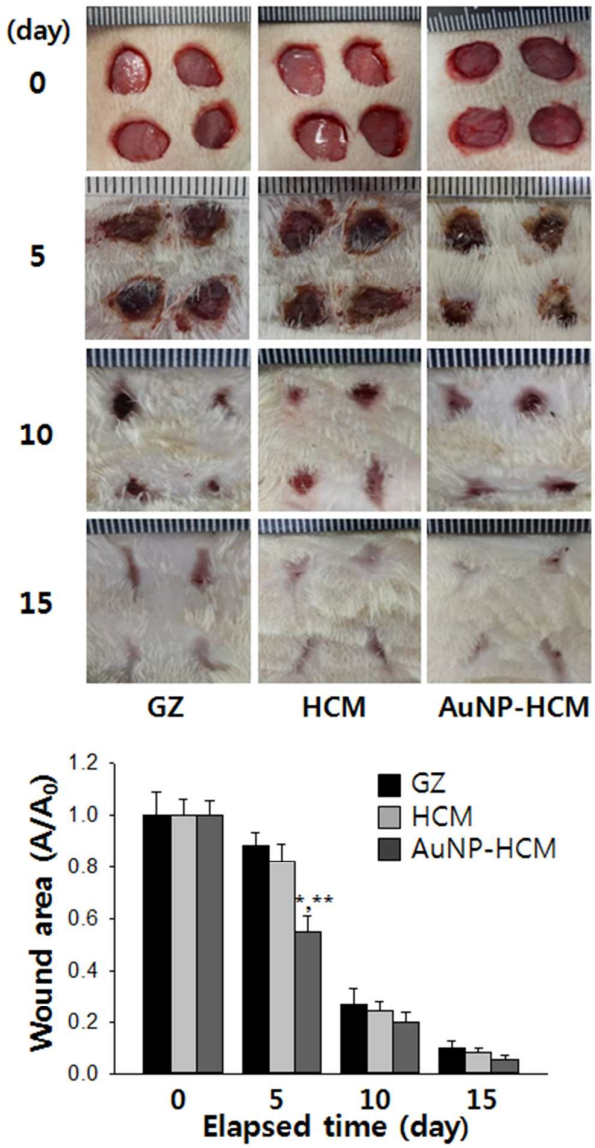
(day)
0
5
10
15
GZ
HCM
AuNP-HCM
Wound area (A/A0)
1.2
1.0
0.8
0.6
0.4
0.2
0.0
GZ
HCM
AuNP-HCM
*,**
0
5
10
15
Elapsed time (day)

Figure 3

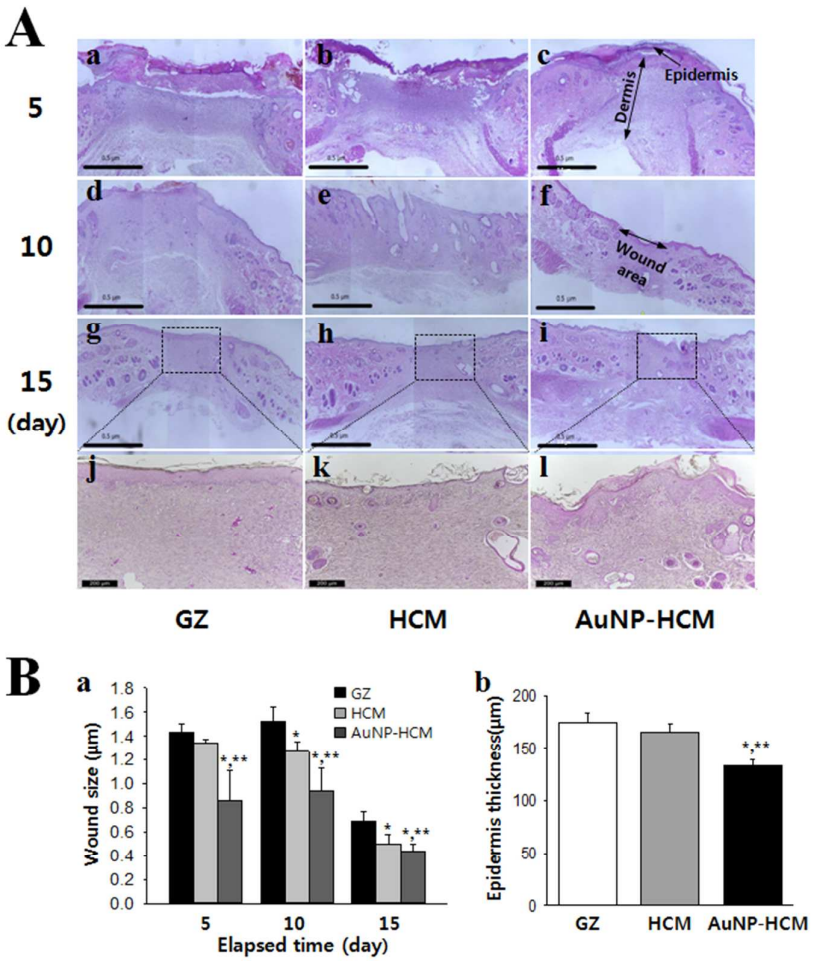
A
5
10
15
(day)
a
b
c
d
e
f
g
h
i
j
k
l
Epidermis
Dermis
Wound area
GZ
HCM
AuNP-HCM
B
a
Wound size (μm)
1.8
1.6
1.4
1.2
1.0
0.8
0.6
0.4
0.2
0.0
GZ
HCM
AuNP-HCM
5
10
15
Elapsed time (day)
b
Epidermis thickness(μm)
200
150
100
50
0
GZ
HCM
AuNP-HCM

Figure 4

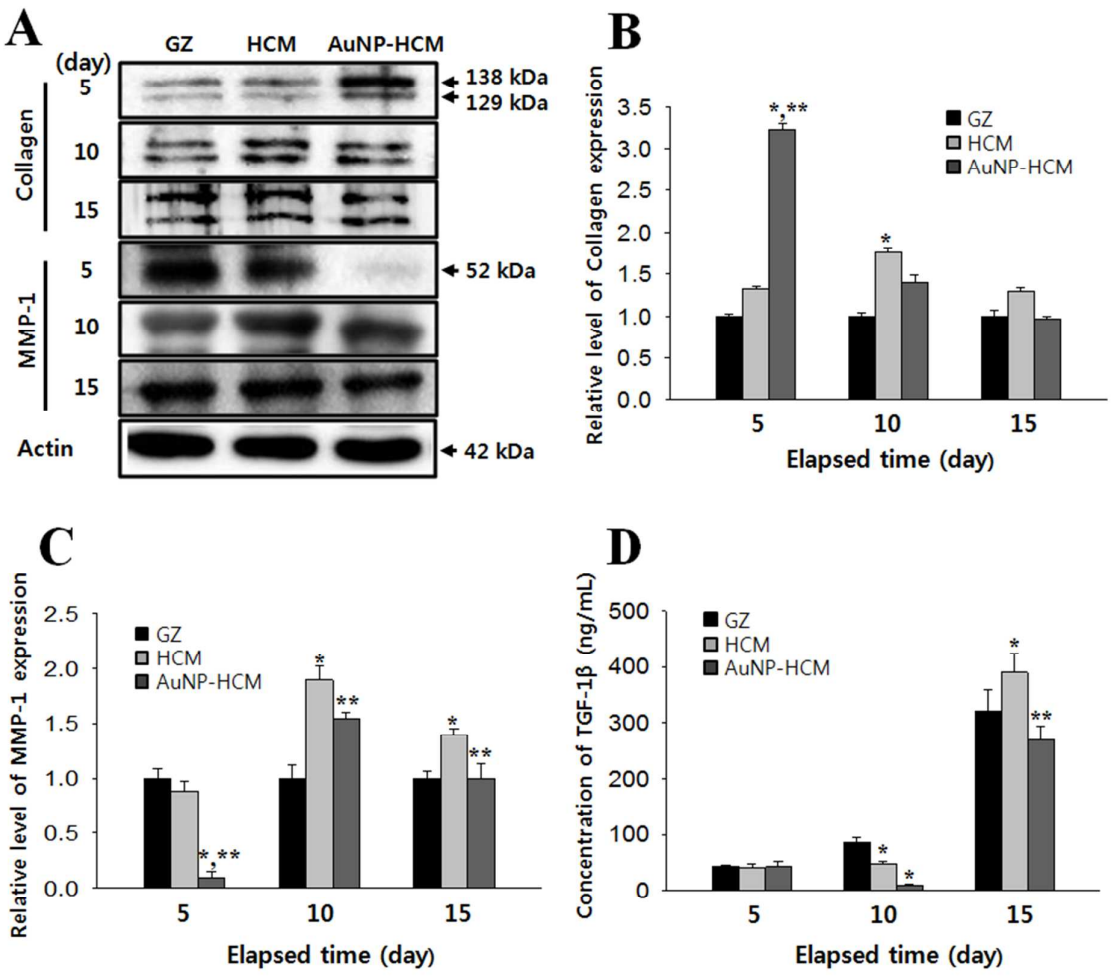
A
GZ
HCM
AuNP-HCM
(day)
Collagen
MMP-1
Actin
5
10
15
138 kDa
129 kDa
52 kDa
42 kDa
B
Relative level of Collagen expression
GZ
HCM
AuNP-HCM
Elapsed time (day)
C
Relative level of MMP-1 expression
Elapsed time (day)
D
Concentration of TGF-1β (ng/mL)
Elapsed time (day)

Figure 5

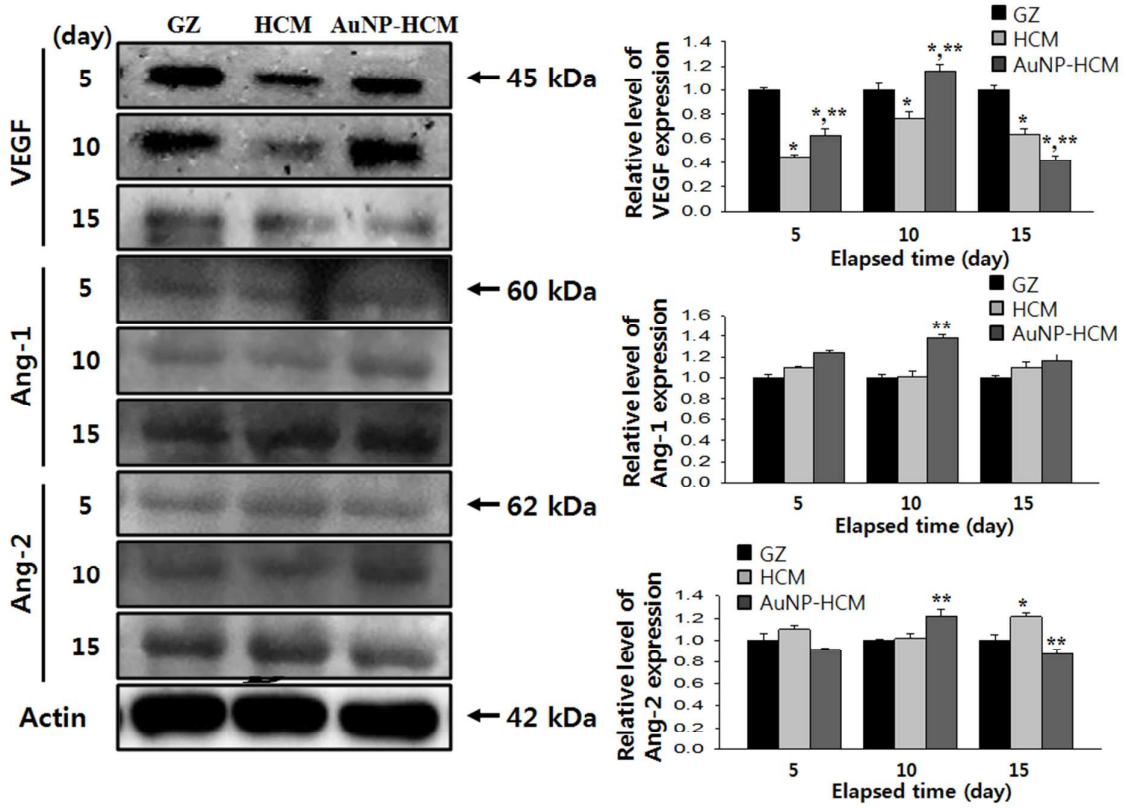
(day)
GZ
HCM
AuNP-HCM
VEGF
Ang-1
Ang-2
Actin
5
10
15
45 kDa
60 kDa
62 kDa
42 kDa
Relative level of VEGF expression
Relative level of Ang-1 expression
Relative level of Ang-2 expression
Elapsed time (day)

Figure 6

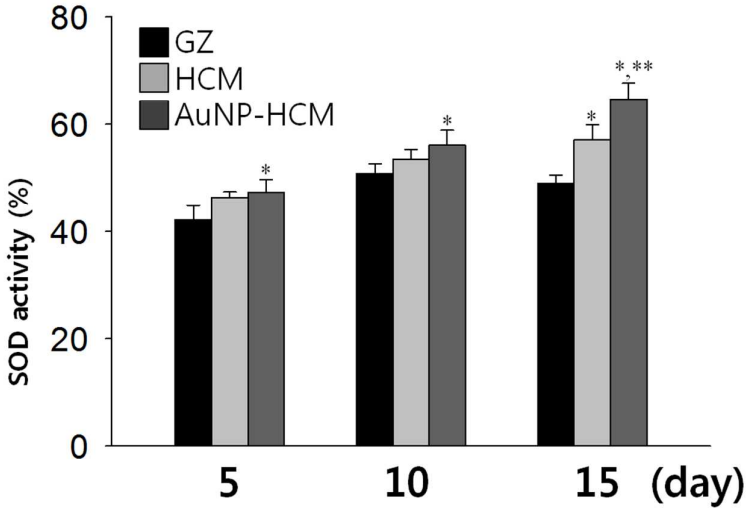

Table 1.

Day	Group	Concentration (mg/dl)					
		ALP	ALT	AST	LDH	BUN	Cr
5	GZ	314±54.11	57.75±6.65	83.75±4.27	221±52.92	13.33±2.57	0.50±0.02
	HCM	308±11.26	64.00±2.16	89.75±7.51	200±85.35	10.53±4.89	0.54±0.02
	AuNP-HCM	335±89.11	53.25±3.77	85.75±3.77	279±99.9	11.10±1.13	0.51±0.01
10	GZ	363±71.13	58.00±2.70	89.75±7.13	177±40.99	19.80±2.24	0.52±0.03
	HCM	342±53.02	53.50±3.51	83.25±3.59	215±37.98	17.07±1.64[a]	0.56±0.02
	AuNP-HCM	346±61.42	46.25±3.77	76.50±9.01	132±33.32	13.55±1.96[a,b]	0.49±0.02
15	GZ	425±52.16	68.50±2.62	90.00±3.14	267±60.96	16.22±1.95	0.58±0.03
	HCM	359±69.07	59.75±2.98	92.25±3.68	291±24.28	15.82±1.80[a]	0.57±0.01
	AuNP-HCM	380±48.36	58.75±3.50	81.50±2.56	269±44.56	13.67±1.45[a,b]	0.57±0.01

* Data represent the mean ± SD from three replicates. a, $p < 0.05$ is the significance level compared to GZ treated group. b, $p < 0.05$ is the significance level compared to HCM treated group.